Concurrent Optimal Re/active Power Control for Wind Farms under Low-voltage-ride-through Operation

Xue Lyu, *Member, IEEE*, Youwei Jia, *Member, IEEE*, Tao Liu, *Member, IEEE*, Yufei He, *Student Member, IEEE*

***Abstract*--A novel concurrent control scheme of optimal re/active power regulation in a wind farm is proposed in this letter, of which the objective is to minimize the detrimental shortfall of active power during low-voltage-fault events. Distinguished from the existing works, the proposed control scheme incorporates an efficient optimization module into the wind turbine controllers. Specifically, it features the merit that the practical feasibility of tracking the resultant references can be ensured via considering multiple constraints in presence of complex wake interactions. Case studies on a permanent-magnet-synchronous-generator based wind farm built in a joint DIgSILENT-MATLAB platform are carried out to demonstrate the effectiveness of the proposed control scheme.**

***Index Terms*--Wind farm, optimal control, reactive power, active power.**

I. Introduction

WITH the rapid growth of wind energy integration, the system robustness against disturbance is weakened. As the installed wind turbines (WTs) connecting to grids through power electronic converters, there is a lack of reactive current contribution and frequency regulation services. To ensure the stable operation of modern power systems with high penetration of wind power, the re/active power from WTs are expected to be controllable to some extent instead of just being a passive "free-runner". For example, the optimal active power regulation of WTs is investigated in [1] from the grid perspective manner. Besides, many grid codes require that WTs should remain connected to the grid and provide a certain amount of reactive current during a low voltage fault.

In most grid codes, the high priority is usually given to the reactive current injection during the low-voltage ride-through (LVRT) period, and hence the active power output would inevitably be reduced. However, the reduction in active power output following a voltage dip may give rise to the frequency drop [2, 3]. This induced frequency drop will become more severe with the increasing share of wind power. In some cases, if the resulting frequency nadir exceeds the acceptable limits, the under-frequency load shedding would be triggered. Now one kind of possible LVRT solutions is to consume the excessive active power via additional resistors, which inevitably leads to un-admirable energy dissipations. Without resorting to the additional resistors, an alternative solution by adjusting the wind turbine operational status (through rotational rotor and pitching components) becomes more promising. This is because 1) the active power can be controllable instead of immediately being interrupted; 2) the excessive energy can be favorably "stored" and conducive to imminent system recovering.

Another important issue for WTs in a wind farm (WF) is that there is a wake behind a WT and the wind will be slowed down after leaving this WT. The aerodynamic coupling between WTs leads to the fact that the operational status of the upstream WTs (i.e. the tip speed ratio and blade pitch angle) would impact the wind experienced by downstream WTs, which in turn influence their active power capture capabilities. These complex interactions cast great challenges to optimally manage the operational status of all wind turbines in the WF. Recently, the wake effect has been taken into account in designing the active power control strategies for WFs (e.g. power maximization, set-point tracking [4, 5]). In contrast, research about the reactive power control strategies is still at its infant stage. Considering the current limit of the WTs' grid side converter, an adaptive *Q-V* scheme is proposed in [6], in which the required reactive power among WTs is allocated in proportion to their available reactive power capacity. Whereas the active power regulation is not considered in [6]. From an optimization point of view, a binary integer optimization problem is formulated in [7] to determine whether the priority should be given to the reactive current injection from WTs or to maintain the active current injection at the pre-fault value during voltage disturbances.

To meet the LVRT requirement and reduce the frequency excursion induced by active power output reduction during

This work was partially supported by the Research Grants Council of the Hong Kong Special Administrative Region under the General Research Fund Through Project No. 17209219, Joint Research Fund in Smart Grid (Grant No. U1966601) under cooperative agreement between the National Natural Science Foundation of China (NSFC) and State Grid Corporation of China (SGCC), Guangdong Basic and Applied Basic Research Fund through Grant No. 2019A1515111173, Dept. of Education of Guangdong Province through Young Talent Program with Grant No. 2018KQNCX223 and High-level University Fund with Grant No. G02236002.

X. Lyu is with the Department of Electrical and Electronic Engineering, Southern University of Science and Technology, Shenzhen, China, and is also with the Department of Electrical and Electronic Engineering, The University of Hong Kong, Hong Kong. (email: xue.lyu@hku.hk)

Y. Jia is with the Department of Electrical and Electronic Engineering, Southern University of Science and Technology, Shenzhen, China. (jiayw@sustech.edu.cn)

T. Liu is with the Department of Electrical and Electronic Engineering, The University of Hong Kong, Hong Kong. (email: taoliu@eee.hku.hk)

Y. He is with the Department of Electrical Engineering, The Hong Kong Polytechnic University, Hong Kong. (email: 3120100780hyf@gmail.com)

LVRT and after fault clearness, an optimal cooperation amongst multiple WTs is needed to improve the control performance of WFs. To this end, a novel control scheme is proposed in this letter, which makes a breakthrough in terms of concurrent re/active power management and wake handling. In the proposed control scheme, an optimization module is newly established in collaboration with WTs' control module. In particular, the optimization module aims to minimize the active power shortfall during LVRT operation and maximize overall wind power production during normal operation. The WTs' control module aims to trace the references generated via the optimization module in real-time. The proposed scheme is technically valid since the existing resources of WTs make it feasible to regulate the re/active power to a certain extent. To further verify the effectiveness of the proposed controller, time-domain simulations are conducted in a joint DIgSILENT-MTALAB platform.

II. The Concurrent Optimal Re/active Power Control Scheme for a Wind Farm

A. *Wind Turbine Model and Wake Effect Model*

In this letter, we consider a WF with n permanent-magnet-synchronous-generator (PMSG)-WTs. The mechanical power of the i-th PMSG-WT, $i = 1, \cdots, n$, that extracts from wind can be expressed as,

$$P_i = \frac{1}{2}\rho A_i C_p(\lambda_i, \beta_i) v_i^3 \tag{1}$$

where ρ denotes the air density; A_i denotes the area swept by the rotor blades of i-th WT; C_p and v_i denotes the power coefficient and the wind speed of the i-th WT, respectively. Specifically, the power coefficient is determined by the tip speed ratio λ_i ($\lambda_i = \omega_{ri} / v_i$, in which ω_{ri} is the rotor speed) and pitch angle β_i.

The wind leaving a WT has a low energy content than the wind arriving in front of the WT due to the wake effect. The Jensen's wake model is adopted in this letter, and the velocity profile of the i-th WT can be expressed as,

$$v_i = v_0 \left\{ 1 - \sum_{j \in n: x_j < x_i} [(1 - \sqrt{1 - C_{Tj}})(\frac{D_i}{D_j + 2kx_{j\to i}})^2 \frac{A_{j\to i}^{shadow}}{A_i}] \right\} \tag{2}$$

where v_0 is the free wind speed; D_i is the blades diameter of the i-th WT; C_{Tj} is the thrust coefficient (which is also determined by the tip speed ratio and pitch angle) of the upstream j-th WT; $x_{j\to i}$ is the distance of upstream WT j and downstream WT i along with the wind direction; $A_{j\to i}^{shadow}$ is the overlap between the area spanned by the wake shadow cone generated by j-thWT and the area swept by the i-th WT; and k is the decay constant.

B. *The WF Central Controller*

a) *LVRT Requirement*

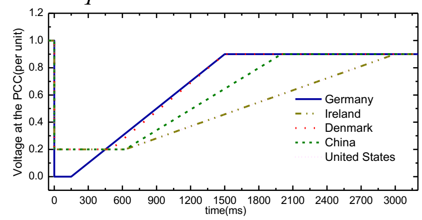

Fig. 1. LVRT requirements for WTs in different countries

Recently, grid codes have introduced the LVRT requirement, which requires that WTs should remain connected to the grid for a specific time duration according to the point of common coupling (PCC) voltage profile. Fig. 1 shows the LVRT requirements in different countries. As indicated in Fig. 1, the ride through time has a slight difference for different countries and WTs are only allowed to disconnect from the grid when the voltage is below the borderline. Meanwhile, a certain amount of reactive current injection from WTs is required during LVRT. The expected reactive current is proportional to the voltage dip, and the proportional coefficient may be set in the range of 0-10. For example, WTs are required to guarantee continuous operation for at least 625 ms when the PCC voltage drops to 20% of the rated value in China; and according to the requirement for WFs interconnection in China [8], the reactive current injection is mathematically expressed as,

$$i_{qWF} = \begin{cases} 0, \ V_{pcc} \geq 0.9V_{pcc}^{nom} \\ \min\{1.5(V_{pcc}^{nom} - V_{pcc})i_{WF}^{nom}, i_{WF}^{nom}\}, 0.2V_{pcc}^{nom} \leq V_{pcc} < 0.9V_{pcc}^{nom} \end{cases} \tag{3}$$

where i_{qWF} denotes the reactive current injection from the WF; V_{pcc} denotes the per-unit PCC voltage; V_{pcc}^{nom} denotes the nominal PCC voltage; and i_{WF}^{nom} denotes the nominal current of the WF.

In most countries, a high priority is given to the reactive current injection from WTs during LVRT and there is no requirement for the active power injection. Now a new control method is introduced in EirGrid [9], in which the active power is given a high priority. Specifically, when low voltage faults occur, the active power injected from WTs should be in proportional to the retained voltage and the reactive current should be in proportional to voltage dip. After fault clearness, grid codes usually require the active power to recover to the pre-fault value with a certain rate or within a certain time.

b) *Re/active Power Control for WTs during Different Modes*

During normal operation, maximizing wind power production is the main goal of the WF owner. Owing to wake interactions, the traditional greedy strategy that each WT operates at their maximum power point tracking (MPPT) mode is no longer the optimal option. Once low voltage faults occur, supplying the required reactive current would be given a high priority. As a consequence, the active power shortfall would be inevitable due to converter current limit, which in turn leads to frequency drop. Besides, the more severe the active power reduction is, the larger the frequency excursion would be, and a longer recovery time would be needed. In this connection, meanwhile fulfilling the LVRT requirement, the main target of the WF becomes to minimize the reduction in active power output during LVRT period, such that the frequency excursion following the fault can be mitigated and the post-event frequency recovering can be facilitated. Similarly, the traditional strategy that allocates the same reactive power support task to each WT is no longer the optimal solution. To improve control performance of the WF under these two different situations, a centralized control method is adopted in this work at the WF control layer. A WF central controller will be established to distribute the optimal signal references among WTs after monitoring the PCC voltage and the operational status of individual WTs. To this end, an optimization problem is formulated and is expressed as follows,

$$\min_{\omega_{ri},\beta_i,Q_i\in\mathrm{R}^+} \quad \eta\left(\sum_{i=1}^{n}P_i^{ref}-\sum_{i=1}^{n}P_i^{prefault}\right)^2-(1-\eta)\left(\sum_{i=1}^{n}P_i^{ref}\right) \tag{4}$$

$$\text{s.t.} \quad \sum_{i=1}^{n}Q_i^{ref} = \eta i_{qWF}^{ref}V_{pcc} \tag{5}$$

$$(P_i^{ref})^2+(\eta Q_i^{ref})^2\le(V_{pcc}i_c^{\max})^2 \tag{6}$$

$$0\le\eta Q_i^{ref}\le V_{pcc}i_c^{\max} \tag{7}$$

$$0\le P_i^{ref}\le V_{pcc}i_c^{\max} \tag{8}$$

$$\omega_{ri}^{opt}(\beta_i)\le\omega_{ri}\le\omega_{r\max} \tag{9}$$

$$\beta_{\min}\le\beta_i\le\beta_{\max} \tag{10}$$

According to the different operation modes: the normal mode and LVRT mode, the proposed controller will change its control target accordingly.

Active power maximization during normal operation: If $V_{pcc}\ge 0.9V_{pcc}^{nom}$, $\eta=0$, the WF operates at the power maximization mode. The optimization variables are the rotor speed, and pitch angle of each WT. The notation P_i^{ref} denotes the active power reference of the *i*-th WT.

At the power maximization mode, the effective constraints are (8-10). In particular, the active power reference is subject to (8) due to the converter current limit, where $i_c^{\max}$ denotes the maximum converter current. For WTs rotor speed, according to [10], operating at a rotor speed that lower than $\omega_r^{opt}(\beta)$ (when the wind speed is determined, there exists a rotor speed that achieves the maximum wind power capture at a given pitch angle) may reduce the WT small signal stability margin. Hence to guarantee the stable operation of WTs, the rotor speed variation is limited by (9). The pitch angle variation is constrained by (10). Besides, the wake effect is modelled in (2), where wind speeds reaching to the downstream WTs are calculated according to (2).

Optimal concurrent re/active power control during LVRT: If $0.2V_{pcc}^{nom}\le V_{pcc}<0.9V_{pcc}^{nom}$, $\eta=1$, the WF operates at the LVRT mode. The optimization variables are the rotor speed, pitch angle and reactive power of each WT. The notation Q_i^{ref} denote the reactive power reference of the *i*-th WT, $P_i^{prefault}$ denotes the pre-fault active power output from the *i*-th WT.

At the LVRT mode, the effective constraints of WTs are (5-10). In particular, to satisfy the LVRT requirement, the aggregated reactive power from the WF is constrained by (5). Due to the converter current rating limit, the active and reactive power generation from WTs are constrained by (6-8). Considering the practical operation limits of WTs, the rotor speed and pitch angle variations are constrained by (9) and (10). Since the time duration of the low voltage fault is usually quite short, the free wind speed condition is assumed to remain the pre-fault value during LVRT, and the wake model is also taken into account.

Considering the nonlinearity and non-convexity involved in the formulated optimization problem, the particle swarm optimization algorithm is utilized. The optimization solutions can be solved offline and stored in a look-up table in the WF central controller. Then, online control can be readily achieved.

c) The Wind Turbine Controller

The traditional MPPT control is bypassed and WTs no longer operate at the unity power factor mode to trace the references generated from the optimization module. In particular, the optimized re/active power set-points are sent to the generator side controller module. In addition, different from the MPPT control mode that the pitch controller is only activated when the rotor speed reaches to its upper limit, the optimized pitch angle reference is introduced into the pitch controller. Fig. 2 shows the framework of the proposed control scheme.

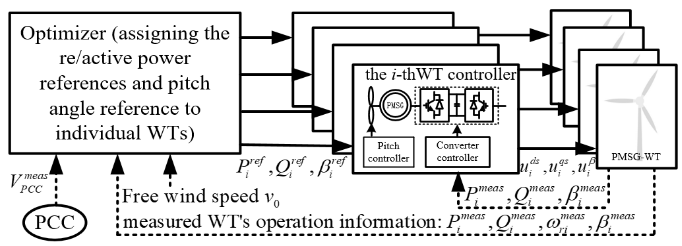

Fig. 2. Framework of the proposed control scheme

III. Case Studies

The configuration of the test system is given in Fig. 3, which includes 4 synchronous generators (SGs) and a 5 MW PMSG-WT based WF. The WF has four rows and each row has four WTs, where the spacing of two adjacent WTs is 5 *D*. Detailed simulation parameters are given in Table I. A DIgSILENT/ MATLAB joint simulation platform is established to verify the proposed control scheme. Specifically, the dynamic model of the test system is built in DIgSILENT, and the optimization module is implemented in MATLAB. The bidirectional data exchange is set up in the joint platform.

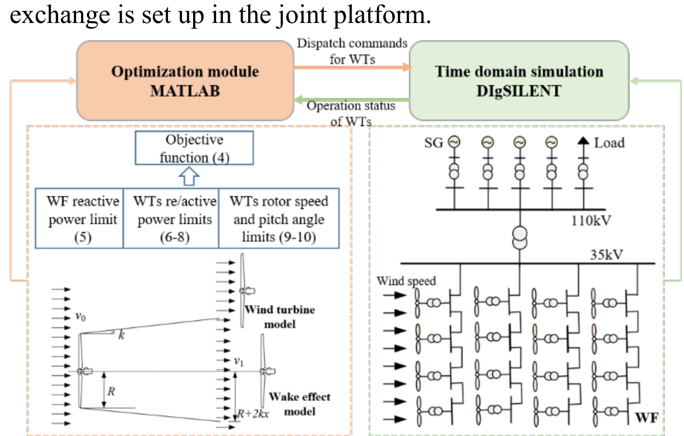

Fig. 3. The joint simulation platform

Table I Parameters of the simulation model

Symbol	Item	Value

i_c^{max}	The maximum WT converter current setting	1.11 p.u.
$\omega_{r\max}$	The maximum WT rotor speed setting	1.2 p.u.
$\beta_{\min}$	The minimum WT blade pitch angle setting	0°
$\beta_{\max}$	The maximum WT blade pitch angle setting	90°
P_{n_SG}	The nominal capacity of SGs	35MVA
μ	Power factor of SGs	0.85

We consider a three-phase symmetric fault that occurs at the PCC bus with the voltage drops to 0.6 p.u.. The fault lasts for 2 s. A constant free wind speed 11 m/s is assumed considering the relatively short duration time of the fault. For comparisons, two different control strategies for the wind farm have been adopted. In the first strategy (Strategy A), each WT operates at their MPPT mode under normal operation, and the reactive power requirement is identically sent to each WT during the LVRT period. The second strategy is the proposed one (Strategy B).

As reported in table II, the WF pre-fault active production increases significantly with the implementation of strategy B than with strategy A. The reduction in active power production during LVRT period is also remarkably mitigated with strategy B. As a result, the incurred frequency excursions can be effectively reduced and the standard frequency deviation throughout simulation is given in table II. The transient time-response curves of the test system are shown in Fig. 4. As shown in Fig. 4(c), the system frequency drops to 49.657 Hz and takes several seconds to recover to the normal value after the fault clearance with Strategy A. In contrast, with Strategy B, the system frequency remains near the nominal value during LVRT period and after fault clearness. It can be found from Fig 4(f) that the WTs in the first, second and third rows operate in a de-loaded mode via increasing their blade pitch angles (i.e. increase to $4.078^{\circ}, 4.591^{\circ}, 3.600^{\circ}$ respectively), such that the spilled energy can be captured by the downstream WTs and the total wind production can be improved. During LVRT period, according to Fig. 4 (b), the reactive power support requirement is met by both strategy A and B. To supply the required reactive power support, the active power output from the first row WTs has to be curtailed with strategy A, and then their blade pitch angle increases to 7.641° to meet this requirement. By comparison, the total variation in WTs' pitch angle during LVRT period is quite small (e.g. the pitch angle of the first row WTs increases by 1.616° and other rows WTs remain unchanged) with strategy B. Simulation results verify that the re/active power generation capabilities from different WTs can be optimally exploited via the proposed control scheme.

Table II Comparison of simulation results with different control strategy

	WF pre-fault active power production	WF active power production during fault	WF reactive power during fault	Standard frequency deviation throughout simulation
Strategy A	42.637 MW	36.319 MW	28.8 MVar	0.107
Strategy B	45.115 MW	44.478 MW	28.8 MVar	0.022

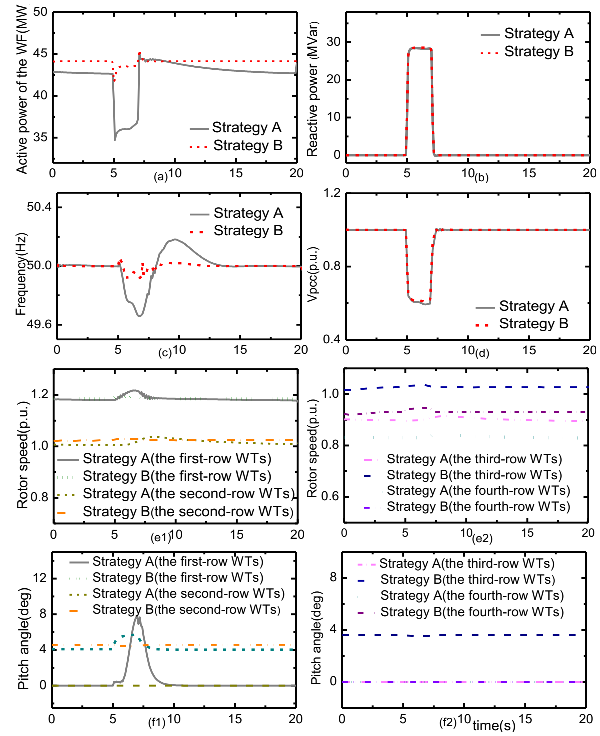

Fig. 4. Simulation results. (a) active power of the WF, (b)reactive power of the WF, (c)system frequency, (d) PCC bus voltage, (e) rotor speed of WTs, (f) pitch angle of WTs.

IV. Conclusion

In this letter, a concurrent re/active optimal control for a WF has been proposed, in which the total active power production from the WF is maximized during normal operation and the aggregated active power shortfall is minimized during low voltage faults. Physical constraints of WTs and the mutual wake interactions have been comprehensively considered in managing wind power sharing. Simulation results have demonstrated that the proposed scheme leads to promising control performance for a WF under LVRT operation.

V. References

[1] X. Lyu, Y. Jia, Z. Xu, and J. Østergaard, "Mileage-responsive Wind Power Smoothing," *IEEE Transactions on Industrial Electronics,* vol. 67, no. 6, pp. 5209-5212, 2019.

[2] J. O'Sullivan, A. Rogers, D. Flynn, P. Smith, A. Mullane, and M. O'Malley, "Studying the maximum instantaneous non-synchronous generation in an island system—Frequency stability challenges in Ireland," *IEEE Transactions on Power Systems,* vol. 29, no. 6, pp. 2943-2951, 2014.

[3] Z. Rather and D. Flynn, "Impact of voltage dip induced delayed active power recovery on wind integrated power systems," *Control Engineering Practice,* vol. 61, pp. 124-133, 2017.

[4] A. S. Ahmadyar and G. Verbič, "Coordinated operation strategy of wind farms for frequency control by exploring wake interaction," *IEEE Transactions on Sustainable Energy,* vol. 8, no. 1, pp. 230-238, 2016.

[5] X. Lyu, Y. Jia, and Z. Xu, "A novel control strategy for wind farm active power regulation considering wake interaction," *IEEE Transactions on Sustainable Energy,* vol. 11, no. 2, pp. 618-628, 2019.

[6] H. Karbouj and Z. H. Rather, "Voltage control ancillary service from wind power plant," *IEEE Transactions on Sustainable Energy,* vol. 10, no. 2, pp. 759-767, 2018.

[7] H. Karbouj and Z. H. Rather, "A novel wind farm control strategy to mitigate voltage dip induced frequency excursion," *IEEE Transactions on Sustainable Energy,* vol. 10, no. 2, pp. 637-645, 2018.

[8] "Technical Rule for Connecting Wind Farm to Power System, PRC National Standard GB/T 19963-2011." Available online: http://www.gb688.cn/bzgk/gb/newGbInfo?hcno=C0B59C55FD4B287CDF02842D074D1476

[9] "EirGrid Grid Code, Version 7." http://www.eirgridgroup.com/site-files/library/EirGrid/GC_VERSION_7_PUBLISHED_v1.pdf (accessed 2018).

[10] N. A. Janssens, G. Lambin, and N. Bragard, "Active power control strategies of DFIG wind turbines," in *Power Tech, 2007 IEEE Lausanne*, 2007: IEEE, pp. 516-521.